JOURNAL OF MATERIALS SCIENCE 27 (1992) 4061–4069

Monte-Carlo simulation on notched strength of unidirectional boron–aluminium composites

SHOJIRO OCHIAI, KOZO OSAMURA
Department of Metallurgy, Kyoto University, Sakyo-ku, Kyoto 606, Japan

A Monte-Carlo simulation was carried out on the fracture behaviour of centre-notched unidirectional boron–aluminium composites assuming quasi self-similar notch extension. The main results obtained in this work are summarized as follows: (i) the experimental results for notched strength of Awerbuch and Hahn and those of Poe and Sova could be described well by the present simulation method; (ii) the notched strength decreased with increasing notch size for a fixed width of specimen and with increasing width of specimen for a fixed relative notch size; (iii) the semi-empirical failure criteria proposed by Waddoups, Eisenman and Kaminski, Whitney and Nuismer, and Mar and Lin could approximately describe the notched strength obtained by the present simulation method under limited conditions, despite the difference in basic concept between these models and the present method; and (iv) the characteristic lengths in the models of Waddoups, Eisenman and Kaminski, and Whitney and Nuismer, which were originally assumed to be material constants, were dependent on notch size and width of specimen. It was demonstrated that these characteristic lengths have a strong positive correlation with damage zone size.

1. Introduction

In notched unidirectional metal-matrix composites, various events such as yielding of the matrix or splitting and breakage of fibres occur at the notch tip. Among the events, yielding of the matrix and splitting have been known to reduce the stress concentration factor in the fibres ahead of the notch tip, from the calculation results based on shear-lag analysis [1–5]. Concerning the breakage of fibres ahead of the notch tip, Reedy [2] and Dharani *et al.* [4] have found in boron–aluminium composite that some fibres ahead of the notch tip are broken prior to a failure of the composite as a whole, and stable notch extension occurs.

The breakage of fibres at the notch tip is influenced by the strength and its scatter in fibres and by the stress concentration factor in the fibres, since breakage occurs when the product of applied stress and the stress concentration factor exceeds the strength of the fibres. However, until now, the influence of the scatter in strength of fibres on the breakage has not been studied, despite the fact that fibres show a scatter in strength in practical composites. In addition to scatter in the strength of fibres, yielding, splitting, notch size and width of the specimen affect the breakage since they affect the stress concentration factor at the notch tip [1–5].

In the present work, the way in which the yielding of matrix, notch size and width of specimen affect the fracture behaviour of centre-notched unidirectional boron–aluminium composite was studied by means of a computer-aided Monte-Carlo simulation method. In this simulation work, the case where no splitting occurs and quasi self-similar (co-planar) notch extension occurs was taken up. This is not the case for weakly bonded composites, since splitting occurs in such composites, which does not allow the self-similar extension of the notch [6, 7]. However, no splitting has been observed in fully annealed boron–6061-0 aluminium composite, and only a small splitting has been observed in boron–6061-T6 composite with long notches [8]. The present simulation can be approved for such cases, to a first approximation.

In this work, simulation experiments were carried out for three samples as shown in Table I. Section 3.1 describes simulation experiments carried out for the data reported by Awerbuch and Hahn [9] (sample 1) and Poe and Sova [10] (sample 2), and the simulation results are compared with the reported data. Section 3.2 describes simulation experiments carried out for various notch sizes and widths of specimen using sample 3, and in Section 3.3 the results are compared with predictions based on the semi-empirical models proposed by Waddoups *et al.* [11], Whitney and Nuismer [12, 13] and Mar and Lin [14, 15].

2. Model and procedure for Monte-Carlo simulation

2.1. Modelling

Recent work [1] has shown that a rough estimation of the notched strength of a composite, σ_N, can be made if the value of fibre strength at the notch tip, σ_{fu}, is properly determined. In this estimation, σ_N was given by $\sigma_f V_f$ in which V_f is the volume fraction of fibre and

TABLE I Mechanical properties of fibre and matrix, and geometrical factors of boron-aluminium composites, on which simulation experiments were carried out

Property	Sample 1 (Awerbuch and Hahn [9])	Sample 2 (Poe and Sova [10])	Sample 3 (present work)
Young's modulus of fibre, E_f (GPa)	475	475	475
Volume fraction of fibre, V_f	0.5	0.5	0.5
Diameter of fibre, d_f^0 (μm)	142	142	142
Average strength of fibre at notch tip (GPa)	4.2	3.5	3.5
Weibull shape parameter for fibre strength	10	10	10
Shear modulus of matrix, G_m (GPa)	27	27	27
Shear yield stress of matrix, τ_y (MPa)	42.7	42.7	50
Strain hardening coefficient of matrix (normalized with G_m), β	0.007	0.007	0.01
Notch length, $2c_0$ (mm)	0–12.85	0–50.8	0–50
Width of sample, W (mm)	25.4	19.1–101.6	10–100
Relative notch length	0–0.5	0–0.5	0–0.7

σ_f is the fibre stress at infinity, satisfying

$$K_2\sigma_f = \sigma_{fu} \quad (1)$$

where K_2 is the stress concentration factor in the fibres at the shoulder of the rectangular notch. Fig. 1 shows a comparison of the calculation results (solid curve) with the experimental data (circles) of Awerbuch and Hahn [9]. The values used in the calculation are listed in Table I, in which the coefficient β of strain-hardening of the matrix, normalized with respect to the shear modulus G_m of the matrix, was chosen to fit the measured load–COD curves [1]. In their specimens, notches 1.27 to 12.7 mm long ($2c_0$) and 0.25 mm wide (2Δ) were introduced by electro-discharge machining. Examining the influence of the magnitude of 2Δ on the strength of the composite, we have found that in this composite system, 0.25 mm of 2Δ could be regarded as small, as shown by the dashed curve in Fig. 1; namely, even if 2Δ was taken to be zero or the notch was assumed to be sharp enough, the resultant strength was not so very different from the strength for $2\Delta = 0.25$ mm. Thus, in the present work, the notch was regarded as sharp and 2Δ was taken to be zero, which made the simulation program simple without a large loss of accuracy.

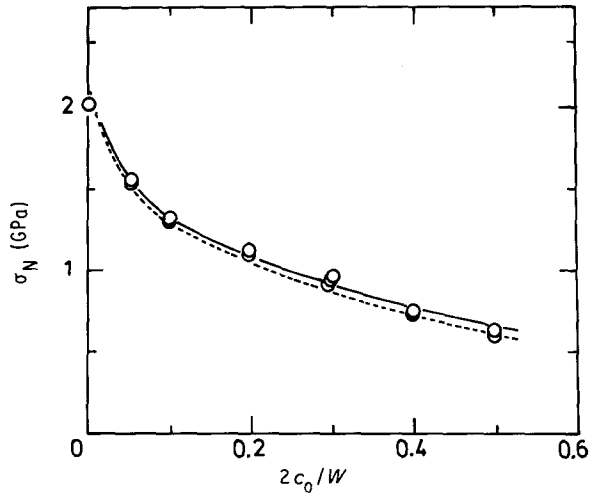

Figure 1 Comparison of calculation results for (——) $2\Delta = 0.25$ mm and (– – –) $2\Delta = 0$ with (○) experimental results obtained by Awerbuch and Hahn [9]. $\sigma_{fu} = 4.2$ GPa, $\beta = 0.007$.

Fig. 2a shows a schematic representation of a transverse cross-section of the composite, in which the fibre array is assumed to be a square one. This three-dimensional composite was converted to a two-dimensional one, as shown in Fig. 2b, whose longitudinal section is shown in Fig. 2c. In this conversion, the

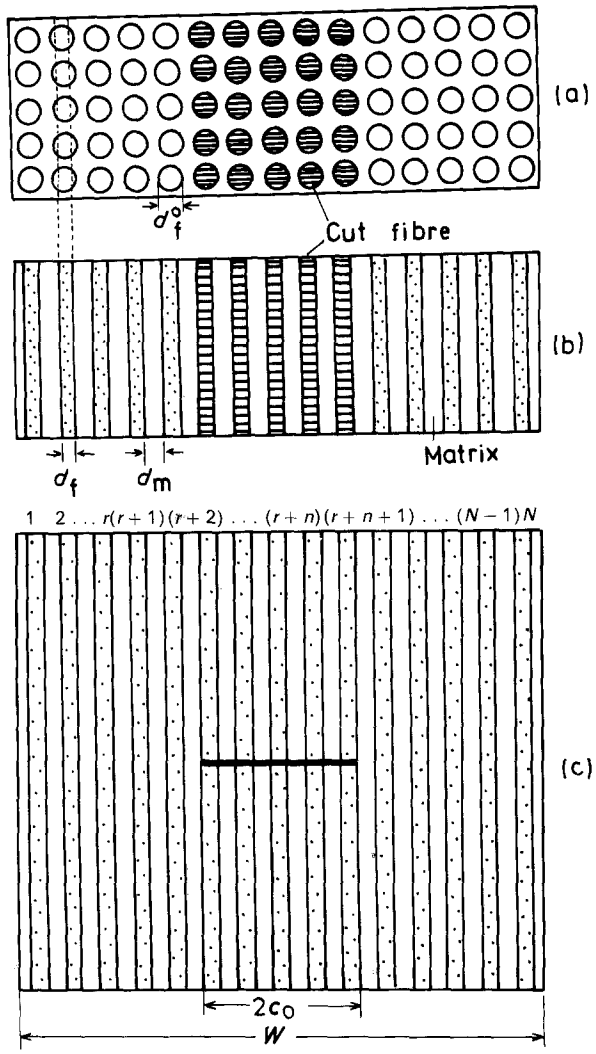

Figure 2 Simplification of configuration of composite from (a) three to (b, c) two dimensions. (a) and (b) show the transverse cross-section in three- and two-dimensional composites, respectively, and (c) shows the longitudinal cross-section in a two-dimensional composite. The hatched fibres in (a) and (b) show cut fibres.

width of the fibre in the two-dimensional model, d_f, was given by

$$d_f = d_f^0 (\pi V_f/4)^{1/2} \quad (2)$$

where d_f^0 is the diameter of the real fibre and V_f is the volume fraction of fibre. The width of the matrix region in the two-dimensional model, d_m, is given by

$$d_m = d_f V_m/V_f \quad (3)$$

where V_m is the volume fraction of matrix.

The present two-dimensional model consists of a total number N of fibres, among which n fibres are cut by the introduction of the centre-notch with a length $2c_0$, as shown in Fig. 2c. Noting the width of the model composite as W, the relation of W to N is expressed as $W = N(d_f + d_m)$, and that of $2c_0$ to n as $2c_0 = nd_f + (n-1)d_m$. N and n in the present two-dimensional model correspond to $h(N/d_f^0)(4V_f/\pi)^{1/2}$ and $h(n/d_f^0)(4V_f/\pi)^{1/2}$ in real three-dimensional composites, where h is the thickness of the composite.

The simulation experiment was carried out by the following procedure, assuming that self-similar notch extension occurs. The contribution of matrix stress to composite stress was neglected, since the fibre stress was about 40 times higher than the matrix stress in the present work.

2.2. Procedure of Monte-Carlo simulation

1. The fibres were numbered as 1 to N from the right to left as shown in Fig. 2c. The fibres from $(r+1)$ to $(r+n)$ in Fig. 2c are cut ones.

2. The stress concentration factor for the fibres ahead of the notch tip was calculated by modifying the method presented in our preceding work [1]. The modification was done in order to express the situation arising during the fracture process. For instance, when the fibre r or $(r+n+1)$ in Fig. 2c just ahead of the notch was broken, n was made $(n+1)$, and when the fibre $(r-1)$ or $(r+n+2)$ was broken prior to the fibre r or $(r+n+1)$, respectively, the boundary conditions were changed to express this condition.

3. The strength of fibre σ_{fu} was assumed to obey the two Weibull distribution functions [16]. The Weibull shape parameter m for boron fibres embedded in 6061 aluminium has been reported by Wright and Will [17] to be 9.93 for 50.8 mm gauge length and 10.94 for 25.4 mm gauge length. m was therefore taken to be 10 in this work. The average strength of the fibres ahead of the notch tip, σ_{fu}, was taken to be 4.2 GPa for sample 1 (Awerbuch and Hahn's composite) and 3.5 GPa for sample 2 (Poe and Sova's composite) from our preceding work [1]. For sample 3, σ_{fu} was taken to be 3.5 GPa.

The strength of the ith fibre $S(i)$ ($i = 1$ to r and $r+n$ to N) was determined by generating a random value R_i and setting $R_i = P$ where P is the cumulative Weibull distribution function for fibre strength. The strength of cut fibres ($i = r+1$ to $r+n$) was set to be zero.

4. Load L_c was applied to the composite, corresponding to the fibre stress at infinity $\sigma_f = L_c/N$, and the stress concentration factor K for each fibre ahead of the notch tip was calculated. When the exerted stress $K\sigma_f$ was lower than the fibre strength, no fibre was broken. The load was then, raised in a step of $\Delta L_c = N\Delta\sigma_f$, where $\Delta\sigma_f$ is the increment in fibre stress at infinity, which was taken to be 10 MPa in this work.

5. When $K\sigma_f$ exceeded the strength of the fibre, the corresponding fibre was regarded as being broken and then its strength was set to be zero. For instance, if fibre r was broken, then $S(r)$ was set to be zero.

6. For the new number of cut fibres, the K values were calculated and it was examined if the fibres could be broken further or not under the new K values. When there occurred further breakage of fibres, again the K values were calculated for the increased number of broken fibres and again it was examined if the remaining fibres could be broken or not. This process was repeated until no further breakage of fibres occurred at a given applied load. If all fibres were broken, the composite was regarded to be broken as a whole.

7. If the fibres were not broken further at the given applied load, the load on the composite L_c was raised step by step and the K values were calculated at each step and procedure 6 was repeated until the composite was broken as a whole.

8. As, in most cases, the notch extended stably until it extended catastrophically, the number of fibres ahead of the initial notch during stable notch extension was also counted. This stable notch extension was considered to correspond to the formation of a damage zone.

The values employed for samples 1 to 3 are summarized in Table I. The simulation experiments were carried out more than 20 times for each condition and the results were averaged.

3. Results and discussion

3.1. Simulation experiments for sample 1 and sample 2

The results of simulation experiments are superimposed in Figs 3 and 4 where the experimental results of Awerbuch and Hahn [9] (sample 1) and Poe and Sova

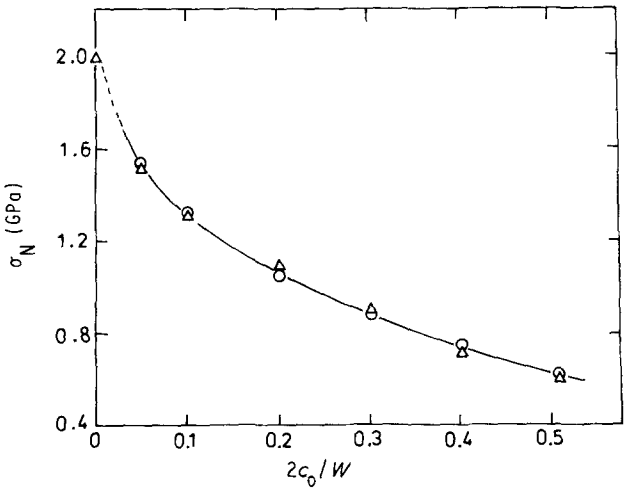

Figure 3 Comparison of the experimental results on σ_N of (△) Awerbuch and Hahn [9] (sample 1) with (○) the results of the present simulation.

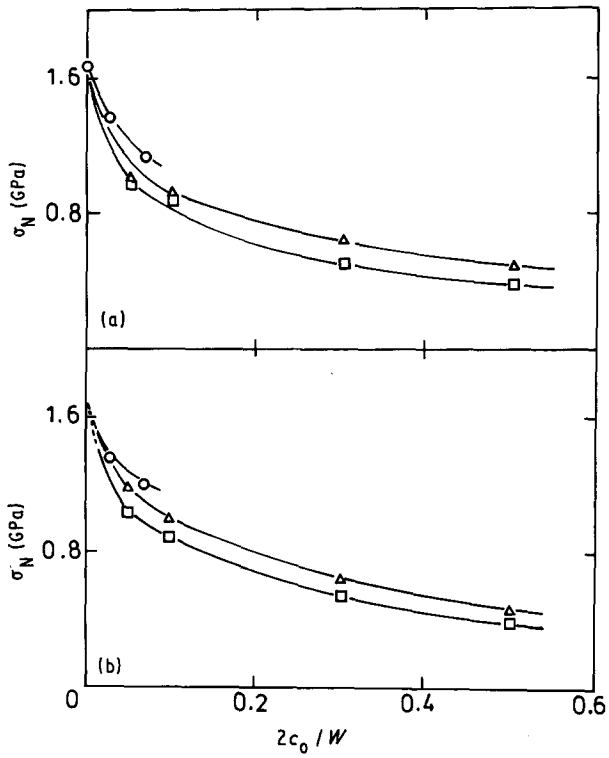

Figure 4 Comparison of (a) the experimental results on σ_N of Poe and Sova [10] (sample 2) with (b) the results of the present simulation. W = (○) 19.1, (△) 50.8, (□) 101.6 mm.

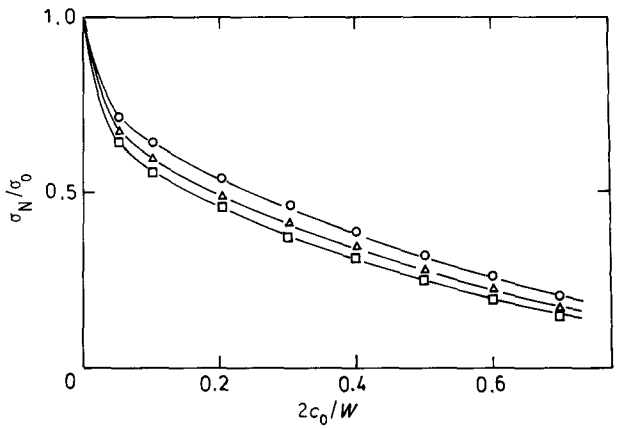

Figure 5 Variation of σ_N/σ_0 as a function of $2c_0/W$ for W = (○) 19.2, (△) 38.5 and (□) 57.7 mm obtained by the simulation for sample 3.

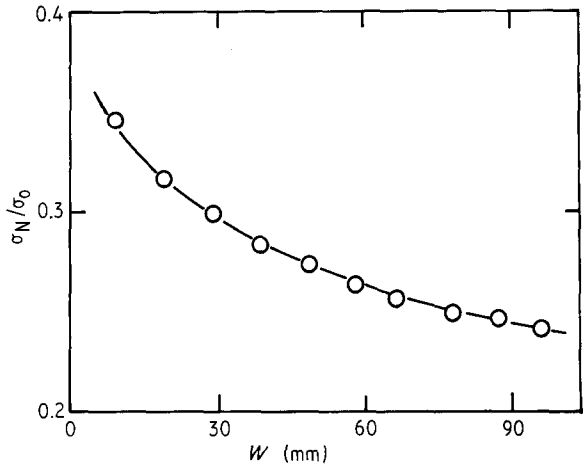

Figure 6 Variation of σ_N/σ_0 as a function of W for $2c_0/W = 0.5$ obtained by the simulation for sample 3.

[10] (sample 2) are shown, respectively. The simulation results show good agreement with the reported data.

The good agreement, however, does not mean that the present method can predict the notched strength in a quantitative manner, due to the arbitrary conversion from a three- to a two-dimensional composite, and due to the choice of properly determined values of σ_{fu}. Within the accuracy of the present work, it can be noted that the present method can, at least, predict the right trends and can yield good agreement when properly determined values are chosen for the simulation experiment.

3.2. Influence of notch size and width of specimen on notched strength for sample 3

In this and the following sections, the simulation experiments were carried out on sample 3. Fig. 5 shows the variation of notched strength σ_N normalized with respect to σ_0, which was taken to be 1.75 GPa ($= \sigma_{fu}V_f$), as a function of relative notch length ($2c_0/W$) for W = 19.1, 38.5 and 57.7 mm. σ_N/σ_0 decreases with increasing $2c_0/W$ for any value of W, but the reduction in σ_N/σ_0 is large for large W. Fig. 6 shows the variation of σ_N/σ_0 as a function of W under a fixed relative notch length $2c_0/W = 0.5$, indicating that σ_N/σ_0 decreases with increasing W. The tendency that wide specimens have a low σ_N/σ_0 is the same as that of the experimental results of Poe and Sova [10], as shown in Section 3.1.

3.3. Comparison with the predictions of other models

Until now, various kinds of technique and various failure criteria have been employed to describe the notched strength of unidirectional and cross-plied composites. For this situation, Awerbuch and Mudhukar [18] mentioned the following reasons: different composite systems demonstrate different failure modes and damage mechanisms at the notch tip and may require correspondingly different analytical tools and experimental techniques, and there is not yet a consensus regarding the proper set of criteria for failure. Due to the multiplicity of failure modes and the corresponding complexity of the failure process and damage progression, a variety of analytical techniques have been developed ranging from comprehensive numerical methods to simplified semi-empirical fracture models. Awerbuch and Mudhukar [18] collected numerous reported experimental results and analysed them with the semi-empirical models proposed by Waddoups *et al.* [11], Whitney and Nuismer [12, 13], Karlak [19], Pipes *et al.* [20–22], Mar and Lin [14, 15], Poe and Sova [10] and others. As a result, they showed that very good agreement between all these fracture models and all experimental notched-

strength data can be established provided the parameters which are employed in the models are properly determined. Their result indicates that, although each model is based on a different concept, each model can describe the experimental results. This could be attributed partly to the semi-empirical nature of the models, which use proper values of the parameters determined by fitting.

In the present work, among the models, the models of Waddoups, Eisenman and Kaminski (the WEK model) [11], Whitney and Nuismer (the WN model) [12, 13] and Mar and Lin (the ML model) [14, 15] were taken as representative and applied to the present results to examine whether these models can describe the present results. The concepts of these models are briefly summarized as follows.

3.3.1. The WEK model

Waddoups *et al.* [11] proposed a model based on the linear elastic fracture mechanics (LEFM) concept which assumes an intense energy region with a size a^*, existing perpendicular to the load direction. According to this model, the notched strength for infinite width ($Y\sigma_N$ where Y is the finite-width correction factor), normalized with respect to the unnotched strength (σ_0), $Y\sigma_N/\sigma_0$, is given by

$$\frac{Y\sigma_N}{\sigma_0} = \left(\frac{a^*}{a^* + c_0}\right)^{1/2} \quad (4)$$

3.3.2. The WN model

Whitney and Nuismer [12, 13] considered that the application of LEFM to a composite is questionable, since cracks of the types observed in metals do not form and, unlike metals, a positive correlation between the unnotched strength and fracture toughness seems to exist (namely, the higher the strength, the higher the fracture toughness). They then proposed a model based on the theoretical stress distribution near the notch tip. They assumed that fracture occurs when the stress over some distance d_0 in front of the notch tip is equal to or greater than the unnotched strength (point stress criterion), or when the average stress over some distance a_0 is equal to or greater than the unnotched strength (average stress criterion). d_0 and a_0 are regarded as material constants. According to the point- and average-stress criteria, $Y\sigma_N/\sigma_0$ is given by

$$\frac{Y\sigma_N}{\sigma_0} = (1-\zeta_1^2)^{1/2} \quad (5)$$

$$\frac{Y\sigma_N}{\sigma_0} = \left(\frac{1-\zeta_2}{1+\zeta_2}\right)^{1/2} \quad (6)$$

respectively, where ζ_1 and ζ_2 are given by $c_0/(c_0 + d_0)$ and $c_0/(c_0 + a_0)$, respectively. For centre-notched specimens, a^* in the WEK model is related to the characteristic length a_0 for the average stress criterion by $a^* = a_0/2$ from a comparison of Equation 4 with Equation 6. Although these models are based on different concepts, they are operatively equivalent [20].

3.3.3. The ML model

Mar and Lin [14, 15] proposed that fracture of the composite for mode I is given by

$$Y\sigma_N = H_c(2c_0)^{-w} \quad (7)$$

where H_c is the composite toughness which has the dimension of [stress] × [(length)^w] and the exponent w is a parameter related to the strength of the singularity at the notch tip. Equation 7 can be compared with

$$Y\sigma_N = K_{Ic}(\pi c_0)^{-1/2} \quad (8)$$

based on the LEFM approach, where K_{Ic} is the critical stress intensity factor. In their model, the discontinuity was modelled at its tip as if it were a notch with its tip at the interface of a bi-material, i.e. the matrix and fibre. This model pictures the notch as being in matrix-type material poised to propagate into fibre-type material. In this model, w was calculated to be 0.34 for a boron–aluminium composite.

3.3.4. Application of WEK and WN models to the simulation results for sample 3

For the finite width correction factor, Y, Fedderson's expression [23] given by

$$Y = [\sec(\pi c_0/W)]^{1/2} \quad (9)$$

was used. As a_0 for the average stress criterion of the WN model is equal to $2a^*$ for the WEK model, a^* was used as the representative of a_0 and a^*. Rearranging Equations 4 and 5, gives

$$c_0 = a^*\left[\left(\frac{\sigma_0}{Y\sigma_N}\right)^2 - 1\right] \quad (10)$$

for the WEK model and

$$c_0 = d_0\left\{\left[1 - \left(\frac{Y\sigma_N}{\sigma_0}\right)^2\right]^{-1/2} - 1\right\}^{-1} \quad (11)$$

for the point-stress criterion of the WN model. Since a^* and d_0 are assumed to be material constants, being independent of notch size, c_0 should be proportional to $(\sigma_0/Y\sigma_N)^2 - 1$ for the WEK model and to $\{[1 - (Y\sigma_N/\sigma_0)^2]^{-1/2} - 1\}^{-1}$ for the point-stress criterion, respectively. Using average values of σ_N for respective value of c_0, the parameters $(\sigma_0/Y\sigma_N)^2 - 1$ and $\{[1 - (Y\sigma_N/\sigma_0)^2]^{-1/2}\}^{-1}$ were calculated, and c_0 was plotted against these parameters as shown in Figs 7 and 8. The following features could be seen.

(i) For each width of specimen, c_0 is not necessarily proportional to $(\sigma_0/Y\sigma_N)^2 - 1$ and $\{[1 - Y\sigma_N/\sigma_0)^2]^{-1/2}\}^{-1}$ as shown by the solid curves, but, to a first approximation, it could be approximated to be proportional as shown by the broken lines.

(ii) The slopes corresponding to a^* and d_0 in Figs 7 and 8, respectively, are dependent on the width of specimen W. These features suggest that a^* and d_0 could be assumed as constants for a fixed width of specimen to a first approximation, but not as material constants due to the dependency on the width of specimen.

For given widths of specimen, a^* and d_0 were estimated from the slopes. Using these estimated values, the variation of $Y\sigma_N/\sigma_0$ for the respective width

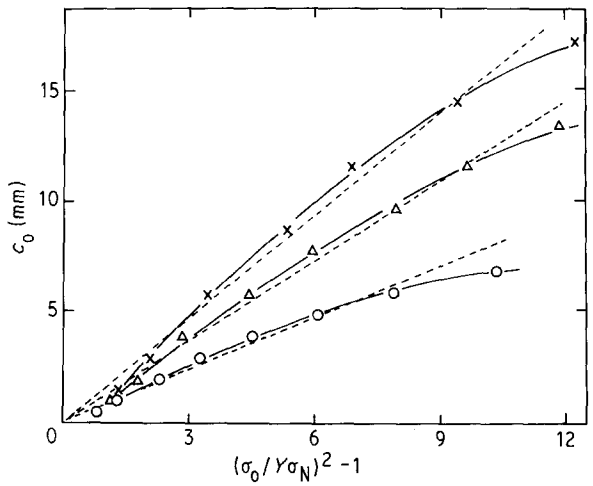

Figure 7 c_0 plotted against $(\sigma_0/Y\sigma_N)^2 - 1$ for $W = (\bigcirc)$ 19.2, $(\triangle)$ 38.5 and $(\times)$ 57.7 mm in sample 3. The values of σ_N/σ_0 are shown in Fig. 5. The solid curves refer to the relations fitted to the results. The broken lines refer to relations based on linear approximations of the results, whose slopes correspond to a^* in the WEK model.

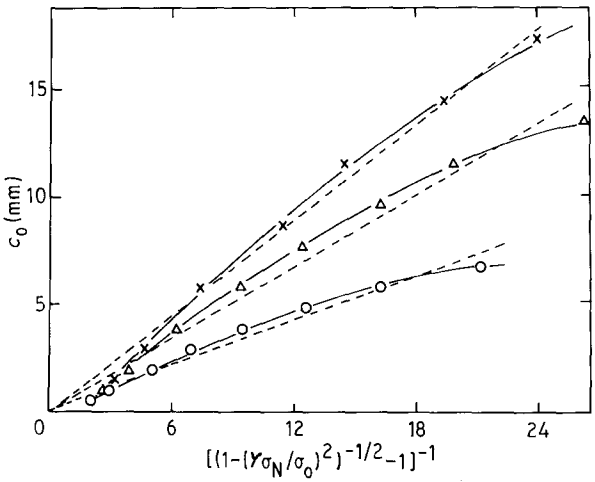

Figure 8 c_0 plotted against $\{[1-(Y\sigma_N/\sigma_0)^2]^{-1/2}\}^{-1}$ for $W = (\bigcirc)$ 19.2, $(\triangle)$ 38.5 and $(\times)$ 57.7 mm in sample 3. The values of σ_N/σ_0 are shown in Fig. 5. The solid curves refer to the relations fitted to the results. The broken lines refer to relations based on linear approximations of the results, whose slopes correspond to d_0 in the point-stress criterion.

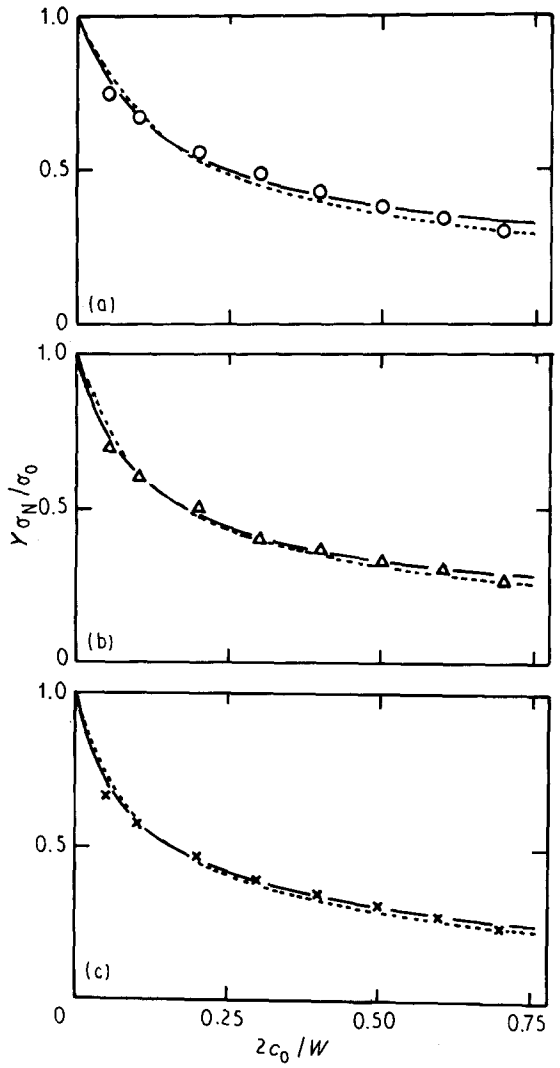

Figure 9 Comparison of the present data for $Y\sigma_N/\sigma_0$ in sample 3 for $W =$ (a) 19.2, (b) 38.5 and (c) 57.7 mm with predictions based on (——) the WEK model and (– – –) the point-stress criterion. The values of a^* and d_0 employed for the predictions were taken from the slopes of the broken lines shown in Figs 7 and 8: (a) (– – –) $d_0 = 0.38$ mm, (——) $a^* = 0.80$ mm; (b) (– – –) $d_0 = 0.60$ mm, (——) $a^* = 1.15$ mm; (c) (– – –) $d_0 = 0.76$ mm, (——) $a^* = 1.52$ mm.

of specimen as a function of $2c_0/W$ was well described as shown in Fig. 9. Thus it could be stated that the WEK and WN models can empirically describe the notched strength under a condition of fixed width of specimen.

However, d_0, a_0 and a^* are originally assumed to be material constants in the WEK and WN models. Therefore they should be independent of the width of specimen. They were, however, not so in the present work. Fig. 10 shows the dependency of a^* and d_0 on width of specimen under a condition of fixed relative notch length $2c_0/W = 0.5$. Within the range in the present work, a^* and d_0 increased with increasing W. Such a tendency has been observed experimentally for cross-plied graphite–epoxy composites [13, 18, 24, 25]. Also for unidirectional boron–aluminium composite, there seems to exist such a tendency as follows.

Applying the WEK model to the data of Poe and Sova [10] shown in Fig. 4a, a^* is calculated to increase from 1.14 mm for $W = 50.8$ mm to 1.43 mm for $W = 101.6$ mm when $2c_0/W = 0.1$, from 1.45 to 1.54 when $2c_0/W = 0.3$ and from 1.35 to 1.45 mm when $2c_0/W = 0.5$. When the WEK model is applied to the results for two-ply composites reported by Goree and Jones [8], a^* increases from 1.03 mm for $W = 25.4$ mm to 1.93 mm for $W = 50.8$ mm and then to 2.11 mm for $W = 73.1$ mm for 6061–0 matrix, and from $a^* = 0.67$ to 0.91 and then 1.42 mm, respectively, for 6061-T6 matrix, where $2c_0 = 3.18$, 9.52 and 15.9 mm for $W = 25.4$, 50.8 and 73.1 mm, respectively. Applying the WN model, d_0 and a_0 show the same tendency as a^*.

Such a width-effect on a^*, d_0 and a_0 is likely to relate to the extensive notch-tip zone size developed prior to catastrophic fracture of a composite as a whole [18]. As has been known, the damage zone plays an important role in fracture performance. The stable crack growth, Δc, corresponding to a damage

zone in the direction perpendicular to the tensile axis was obtained by counting the number of breakages of fibres on left and right sides of the initial notch tip, N_d, and then converting this number of breakages to Δc by the relation

$$\Delta c = (d_f + d_m)N_d/2 \quad (12)$$

Fig. 10 shows the variations of Δc in addition to those of a^* and d_0 as a function of W in the specimens whose notched strength data are shown in Fig. 6. Δc increases with increasing W. This tendency is qualitatively the same as that observed experimentally by Goree and Jones [8].

It is clearly shown in Fig. 10 that Δc increases with increasing W as well as a^* and d_0. The relation of a^* to Δc and that of d_0 to Δc were then examined by using the present data. Figs 11 and 12 show a^* and d_0

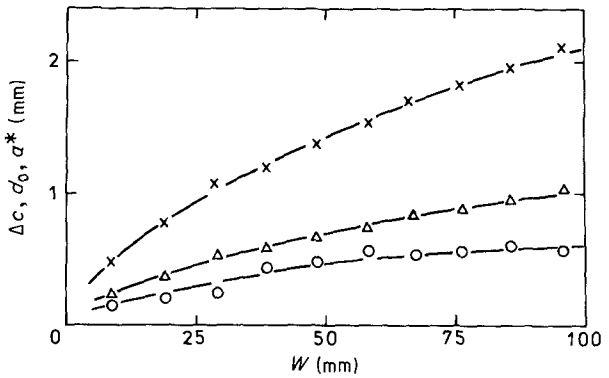

Figure 10 Variations of (○) Δc, (△) d_0 and (×) a^* as a function of W for $2c_0/W = 0.5$ in sample 3. The values of σ_N/σ_0 for these specimens are shown in Fig. 6.

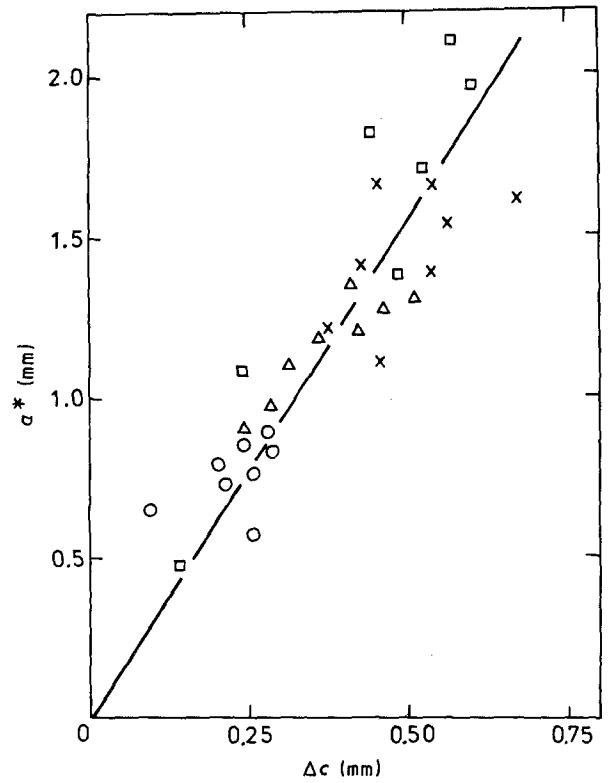

Figure 11 Correlation of a^* with Δc for sample 3: (○) $W = 19.2$ mm, (△) $W = 38.5$ mm, (×) $W = 57.7$ mm, (□) $2c_0/W = 0.5$.

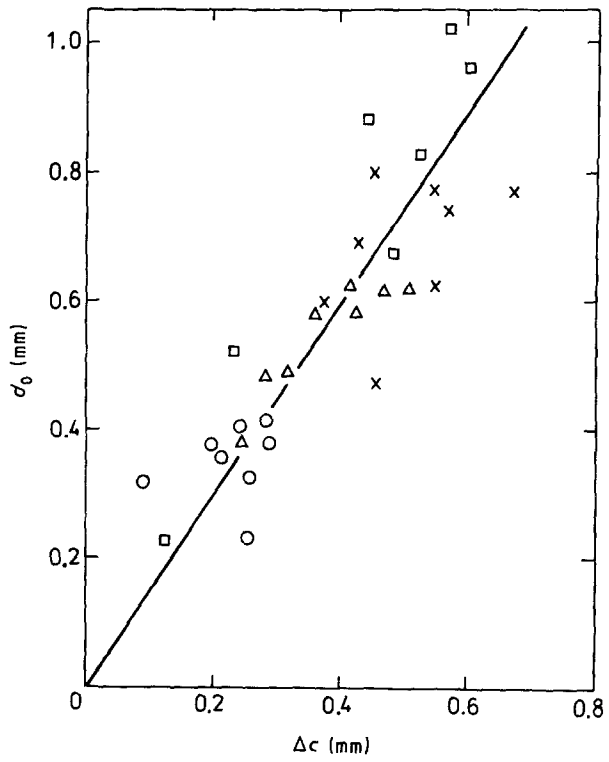

Figure 12 Correlation of d_0 with Δc for sample 3: (○) $W = 19.2$ mm, (△) $W = 38.5$ mm, (×) $W = 57.7$ mm, (□) $2c_0/W = 0.5$.

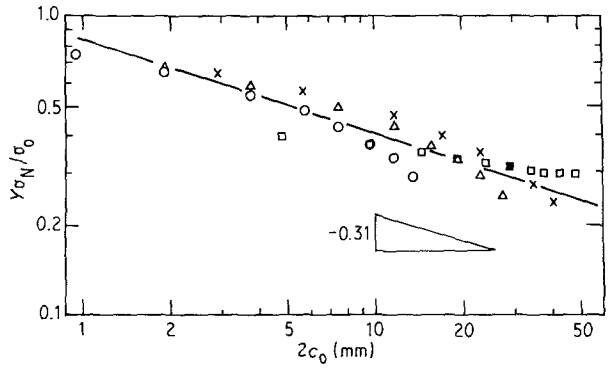

Figure 13 $Y\sigma_N/\sigma_0$ of all sample 3 specimens plotted against $2c_0$ in log–log scale: (○) $W = 19.2$ mm, (△) $W = 38.5$ mm, (×) $W = 57.7$ mm, (□) $2c_0/W = 0.5$.

plotted against Δc, respectively. Although there is a large scatter, there is a tendency that a^* and d_0 are nearly proportional to Δc. These results indicate that the characteristic lengths a^* for the WEK model and d_0 and a_0 for the WN model are dependent on how the damage zone develops. Goree and Jones [8] observed experimentally that the extent of stable notch extension is large when the specimen is wide. As shown above in the analysis of their data based on the WEK model, a^* was large when the specimen was wide. In this way, the relation of d_0 and a^* to Δc obtained in the present work seems to describe right trend.

In this section, it has been shown that the failure criteria of WEK and WN models can describe the notched strength well as a function of notch length when the width of specimen is fixed. On this point, these models are of practical use.

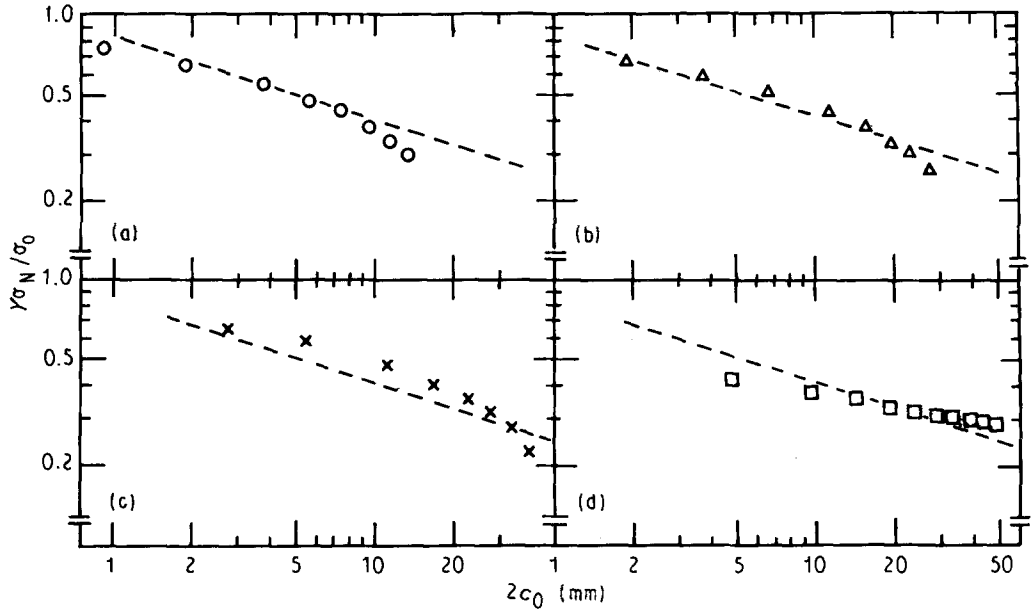

Figure 14 $Y\sigma_N/\sigma_0$ in sample 3 for W = (a) 19.2, (b) 38.5 and (c) 57.7 mm, and (d) for $2c_0/W \simeq 0.5$, plotted against $2c_0$ in log–log scale. The relations of $Y\sigma_N/\sigma_0$ to $2c_0$ given by Equation 13 are shown by broken lines.

3.3.5. Application of ML model

Fig. 13 shows the values of $Y\sigma_N/\sigma_0$ plotted against $2c_0$ in a log–log scale. $\mathrm{Log}(Y\sigma_N/\sigma_0)$ decreases linearly with increasing $\log(2c_0)$ to a first approximation. From the fitting, $Y\sigma_N/\sigma_0$ was expressed as

$$Y\sigma_N/\sigma_0 = 0.84(2c_0)^{-0.31} \quad (2c_0 \text{ in mm}) \quad (13)$$

The parameter w, corresponding to the singularity, was 0.31, which was in good agreement with the predicted value of 0.34 [14, 15]. This indicates that the present notched strength is also described by the empirical equation of the ML model, to a first approximation, although the present result was obtained on the basis of a different concept from that of the ML model.

It should, however, be noted that the ML model cannot necessarily describe the notched strength of the various series of the present work, as shown in Fig. 14. In each series, some deviation from Equation 13 is found. These results indicate that application of the ML model should be done carefully as well as that of the WEK and WN models.

4. Conclusions

The notched strength of a centre-notched unidirectional boron–aluminium composite was studied by means of a Monte-Carlo computer simulation method, assuming quasi self-similar notch extension. The experimental results of Awerbuch and Hahn [9] and Poe and Sova [10] were well described by the present method. It was demonstrated that the notched strength decreases with increasing width of specimen under a fixed relative notch length, which was in agreement with the reported experimental results. Despite the difference in basic concept among WEK, WN and ML models and the present method, these models could describe the present result under limited conditions. The characteristic lengths a^*, d_0 and a_0 of the WEK and WN models were found to have a strong positive correlation with damage zone size.

Acknowledgement

The authors wish to express their gratitude to the Ministry of Education, Science and Culture of Japan for grant-in-aid No. 01 550 549.

References

1. S. OCHIAI, K. OSAMURA, K. TOKINORI, K. NKAKATANI and K. YAMATSUTA, *Met. Trans.* **22A** (1991) 2085.
2. E. D. REDDY Jr. *J. Mech. Phys. Solids* **28** (1980) 265.
3. C. ZWEBEN, *Engng Fract. Mech.* **6** (1974) 1.
4. L. R. DHARANI, W. F. JONES and J. G. GOREE, *ibid.* **17** (1983) 555.
5. J. A. NARIN, *J. Compos. Mater.* **22** (1988) 561.
6. G. A. COOPER and A. KELLY, *J. Mech. Phys. Solids* **15** (1967) 279.
7. W. R. HOOVER and R. E. ALLRED, *J. Compos. Mater.* **8** (1974) 65.
8. G. GOREE and W. F. JONES, NASA Contractor Report 3753 (1983).
9. J. AWERBUCH and H. T. HAHN, *J. Compos. Mater.* **13** (1979) 82.
10. C. C. POE Jr and J. A. SOVA, NASA Technical Paper 1707 (1980).
11. M. E. WADDOUPS, J. R. EISENMAN and B. E. KAMINSKI, J. Compos. Mater. **5** (1971) 446.
12. J. M. WHITNEY and R. J. NUISMER, *ibid.* **8** (1974) 253.
13. R. J. NUISMER and J. M. WHITNEY, "Fracture Mechanics of Composites", ASTM STP 593 (American Society for Testing and Materials, Philadelphia, 1975) p. 117.
14. J. M. MAR and K. Y. LIN, *J. Aircraft* **14** (1977) 703.
15. *Idem., J. Compos. Mater.* **11** (1977) 405.
16. W. WEIBULL, *J. Appl. Phys.* **18** (1951) 293.
17. M. A. WRIGHT and J. L. WILLS, *J. Mech. Phys. Solids* **22** (1974) 161.
18. J. AWERBUCH and M. S. MUDHUKAR, *J. Reinf. Plast. Compos.* **4** (1985) 3.
19. R. F. KARLAK, in Proceedings, "Failure Modes in Composites IV" (Metallurgical Society of AIME, Chicago, 1977) p. 105.

20. R. B. PIPES, R. C. WETHERHOLD and J. W. GILLESPIE Jr, *J. Compos. Mater.* **12** (1979) 148.
21. *Idem., Polym. Engng Sci.* **19** (1979) 1151.
22. *Idem., Mater. Sci. Engng* **45** (1980) 247.
23. C. E. FEDDERSEN, "Plane Strain Crack Toughness Testing of High Metallic Materials", ASTM STP 410 (American Society for Testing and Materials, Philadelphia. 1966) p. 77.
24. S. OCHIAI and P. W. M. PETERS, *J. Mater. Sci.* **17** (1982) 417.
25. *Idem., ibid.* **17** (1982) 2324.

Received 26 March
and accepted 30 July 1991